

Entanglement dynamics under decoherence: from qubits to qudits

André R. R. Carvalho¹, Florian Mintert^{1,2}, Stefan Palzer^{1,*} and Andreas Buchleitner¹

¹*Max-Planck-Institut für Physik komplexer Systeme,*

Nöthnitzer Strasse 38, D-01187 Dresden

²*Department of Physics,*

Harvard University, Cambridge, MA 02138

(Dated: August 11, 2005)

We investigate the time evolution of entanglement for bipartite systems of arbitrary dimensions under the influence of decoherence. For qubits, we determine the precise entanglement decay rates under different system-environment couplings, including finite temperature effects. For qudits, we show how to obtain upper bounds for the decay rates and also present exact solutions for various classes of states.

PACS numbers: 03.67.-a,03.67.Mn,03.65.Yz,03.65.Ud

I. INTRODUCTION

The production of entangled states and the control of their time evolution became a major issue in current research in view of the development of quantum information theory, and all possible applications associated with it. Besides the formidable experimental advances in this direction, there remains a main obstacle which is the fragility of entanglement under the unavoidable interaction with the environment. This coupling of the quantum system with its surroundings, and the consequent decay of entanglement, motivates important questions such as to understand its sources, to identify the characteristic timescales, and, possibly, to find ways to circumvent it.

To devise appropriate strategies for controlling entangled states under the effect of environment interaction, the first step is to acquire a deeper understanding of the dynamics of the decoherence processes themselves. Despite the rapidly increasing experimental interest in this subject, due to the possibility of monitoring entanglement dynamics [1], most of the theoretical work focused on characterizing static properties of entanglement for quantum states [2–5].

Only very recently the question of entanglement decay under environment-induced mixing has been addressed, for some specific states and environment models, and restricted to the case of two qubits [6–8], probably due to the lack of a genuine *and* computable entanglement measure for systems larger than that. Nonetheless, new techniques for the derivation of bounds [9, 10] of concurrence, one possible entanglement measure, recently allowed a systematic study of entanglement dynamics for more general states, including multipartite [11] and multi-level systems.

These higher dimensional systems are of great interest since they can enlarge the perspectives of efficient ap-

plications in quantum information and can also be used to test fundamental aspects of quantum theory. In fact, entangled states of two d -dimensional quantum systems, the *qudits*, can improve measurement resolution [12, 13] and are known to violate local realism more strongly than qubits [14, 15]. Moreover, they can be used for quantum computation [16–19] and also in quantum cryptography protocols [20, 21], which are safer [22, 23] than their qubit counterparts. Despite the importance of such entangled qudits, reflected in the intense activity on their production and manipulation in different experimental setups [24–30], their dynamics under the influence of environment interaction remained unexplored until now.

The paper is organized as follows. In Section II we will briefly recall a recently developed approach for calculating concurrence which allows us to investigate entanglement between systems of arbitrary dimensions. In Section III we will present the different models which describe the interaction of the system with the environment. Section IV is devoted to the analysis of the entanglement decay rates under decoherence processes, starting from the case of bipartite qubits. With the available analytical tools, some, still unknown, features of the decoherence dynamics are presented. The section closes with the analysis of bipartite qudits. A summary of the main results of the paper is presented in the concluding Section V.

II. ENTANGLEMENT MEASURE: CONCURRENCE

In order to follow the environment-induced time evolution of entanglement, one needs a measure which satisfactorily deals with mixed states. A commonly used measure in the context of two qubits is the concurrence [31], defined for pure states as

$$c(\Psi) = \left| \langle \Psi^* | \sigma_y \otimes \sigma_y | \Psi \rangle \right|, \quad (1)$$

where $*$ stands for complex conjugation performed in the standard, computational basis. For mixed states it can

*Permanent address: Fakultät für Physik/FMF, Stefan-Meier-Str. 21, D-79104 Freiburg

be formulated as

$$c(\rho) = \inf_{\{p_i, \Psi_i\}} \sum_i p_i c(\Psi_i), \quad (2)$$

with

$$p_i > 0, \text{ and } \rho = \sum_i p_i |\Psi_i\rangle\langle\Psi_i|. \quad (3)$$

In contrast to most other measures, Eq. (2) can be solved algebraically with the well known solution $c(\rho) = \max\{\lambda_1 - \lambda_2 - \lambda_3 - \lambda_4, 0\}$, in terms of the square roots, λ_i , of the decreasingly ordered eigenvalues of the matrix $\rho(\sigma_y \otimes \sigma_y) \rho^*(\sigma_y \otimes \sigma_y)$.

For higher dimensional systems, we will use the generalization of concurrence given in [32] that coincides - though not obviously - with the original concurrence [31] if restricted to two-level systems. For practical purposes, it is convenient to express concurrence [33, 34] in terms of an operator A acting on the product space $\mathcal{H} \otimes \mathcal{H}$ of two copies of the system, as

$$c(\Psi) = \sqrt{\langle\Psi| \otimes \langle\Psi| A |\Psi\rangle \otimes |\Psi\rangle}. \quad (4)$$

The operator

$$A = \sum_{\alpha} |\chi_{\alpha}\rangle\langle\chi_{\alpha}| \quad (5)$$

is the projector onto the space spanned by the states $|\chi_{\alpha}\rangle$ that are anti-symmetric with respect to the exchange of the copies of either \mathcal{H}_1 or \mathcal{H}_2 , *i.e.*

$$|\chi_{\alpha}\rangle = (|i_k i_l\rangle - |i_l i_k\rangle) \otimes (|j_m j_n\rangle - |j_n j_m\rangle). \quad (6)$$

The states $\{|i_k\rangle\}$ and $\{|j_m\rangle\}$ form, respectively, arbitrary local bases of \mathcal{H}_1 and \mathcal{H}_2 , and α is a label for the multi-index $[k, l, m, n]$.

To extend this construction for the case of mixed states, one should substitute Eq. (4) in the convex-roof, Eq. (2), which can be written, in terms of subnormalized states $|\psi_i\rangle = \sqrt{p_i} |\Psi_i\rangle$, as

$$c(\rho) = \inf_{\{\psi_i\}} \sum_i \sqrt{\langle\psi_i| \otimes \langle\psi_i| A |\psi_i\rangle \otimes |\psi_i\rangle}. \quad (7)$$

Unfortunately, apart from the two-level case where the operator A can be written in terms of a single vector $|\chi\rangle = (|01\rangle - |10\rangle) \otimes (|01\rangle - |10\rangle)$, no exact solutions for Eqs. (2) and (7) are known and, hence, one has to rely on numerical efforts to calculate the concurrence. Also note that numerical solutions of this optimization procedure define only an upper bound for concurrence, since there is no a priori information available on whether the global minimum or just a local one has been reached.

To circumvent this problem, we will use suitable approximations which provide lower bounds of concurrence [9, 10] and not only allow for an efficient numerical approach, but also, in some cases, for exact algebraic solutions. Starting from a decomposition of the

density matrix in terms of pure (subnormalized) states $\rho = \sum_i |\phi_i\rangle\langle\phi_i|$ and from the vectors $|\chi_{\alpha}\rangle$, one can define a set of matrices T^{α} , given by [43]

$$T_{jk}^{\alpha} = \langle\chi_{\alpha}|\phi_j\rangle \otimes |\phi_k\rangle. \quad (8)$$

These are connected to the previously defined operator A through the tensor

$$\mathcal{A}_{jk}^{lm} = \sum_{\alpha} (T_{lm}^{\alpha})^* T_{jk}^{\alpha} = \langle\psi_l| \otimes \langle\psi_m| A |\psi_j\rangle \otimes |\psi_k\rangle. \quad (9)$$

It was shown in [9] that concurrence is bounded from below by

$$c(\rho) \geq \max \left\{ \mathcal{S}_1 - \sum_{i>1} \mathcal{S}_i, 0 \right\}, \quad (10)$$

where the \mathcal{S}_i are the decreasingly ordered singular values of

$$\mathcal{T} = \sum_{\alpha} Z_{\alpha} T^{\alpha}, \text{ with } \sum_{\alpha} |Z_{\alpha}|^2 = 1, \quad (11)$$

that still depend on the choice of the complex parameters Z_{α} . Although any choice provides a lower bound, one might still wish to carry out an optimization over Z_{α} , though now on a much smaller parameter space and with simpler constraints than in Eq. (7). Moreover, also each matrix T^{α} already provides a lower bound, which can be calculated algebraically.

Finally, let us describe an experimentally motivated approach to calculate lower bounds of concurrence, the quasi-pure approximation [10]. Although environmental influences cannot be avoided completely, under typical experimental conditions one deals with states which are, at least initially, *quasi-pure*. This is, they have a single eigenvalue μ_1 which is much larger than all the others, and an approximation based on this condition can be developed. Indeed, using the spectral decomposition $\rho = \sum_i \mu_i |\Psi_i\rangle\langle\Psi_i|$ of the density matrix and the previously defined subnormalized states, one can see that the elements of \mathcal{A} defined in Eq. (9) are proportional to the square roots of the eigenvalues μ_i :

$$\mathcal{A}_{jk}^{lm} \propto \sqrt{\mu_j \mu_k \mu_l \mu_m}. \quad (12)$$

This proportionality and the assumption that $\mu_1 \gg \mu_i$ allows to order the elements of \mathcal{A} in powers of the square roots of μ_i . Keeping only the leading order terms, *i.e.*, \mathcal{A}_{11}^{11} at zero order, \mathcal{A}_{11}^{j1} , \mathcal{A}_{11}^{1j} , \mathcal{A}_{j1}^{11} and \mathcal{A}_{1j}^{11} at first order, and so on, we can approximate \mathcal{A} by

$$\mathcal{A}_{jk}^{lm} \simeq (T_{lm}^{(\text{qp})})^* T_{jk}^{(\text{qp})}, \quad (13)$$

with

$$T_{jk}^{(\text{qp})} = \frac{\mathcal{A}_{jk}^{11}}{\sqrt{\mathcal{A}_{11}^{11}}}. \quad (14)$$

Thus the quasi-pure concurrence can be written as

$$c(\rho) \simeq c_{\text{qp}}(\rho) = \max \left\{ \mathcal{S}_1 - \sum_{i>1} \mathcal{S}_i, 0 \right\}, \quad (15)$$

where the \mathcal{S}_i are the singular values of the matrix $T^{(\text{qp})}$ defined in Eq. (14).

With these tools at hand, entanglement in higher dimensional systems can be explored in a computationally manageable way. We will use them to monitor the entanglement dynamics under different sources of decoherence.

III. ENVIRONMENT MODELS

We start out with the assumption that each subsystem interacts only, and independently, with its local environment and, therefore, any initially entangled state will evolve, in some cases asymptotically, into a separable one. The dynamics of this decoherence process can be described by the master equation

$$\frac{d\rho}{dt} = (\mathbb{1} \otimes \mathcal{L} + \mathcal{L} \otimes \mathbb{1}) \rho, \quad (16)$$

where ρ is the reduced density operator of the system. The interactions of each component of the system with the environment are assumed to be of the same form, represented by the Lindblad operator \mathcal{L} . Under the assumption of complete positivity and Markovian dynamics, the action of \mathcal{L} on ρ reads

$$\mathcal{L}\rho = \sum_i \frac{\Gamma_i}{2} \left(2L_i \rho L_i^\dagger - L_i^\dagger L_i \rho - \rho L_i^\dagger L_i \right). \quad (17)$$

The operators L_i and the rates Γ_i define, respectively, the specific type of the system-environment coupling, and its strength. Various physical situations may arise when a system is coupled to a reservoir: dissipation can take place, noise can be added to the system, or simply loss of phase coherence can occur. All these processes correspond to a suitable choice of the operators L_i in Eq. (17) and lead to entanglement decay, with a rate which is at the focus of this paper.

For two-level systems, the operators L_i can be written in terms of the Pauli matrices. In the case of an interaction with a thermal bath the Lindblad operator reads

$$\mathcal{L}\rho = \frac{\Gamma(\bar{n}+1)}{2} (2\sigma_- \rho \sigma_+ - \sigma_+ \sigma_- \rho - \rho \sigma_+ \sigma_-) + \frac{\Gamma\bar{n}}{2} (2\sigma_+ \rho \sigma_- - \sigma_- \sigma_+ \rho - \rho \sigma_- \sigma_+). \quad (18)$$

In this equation, the first and the second term on the right hand side describe, respectively, decay and excitation processes (mediated by the two-level excitation and deexcitation operators σ_+ and σ_-), with rates which depend on the temperature, here parametrized by \bar{n} , the average thermal excitation of the reservoir. In the zero

temperature limit, $\bar{n} = 0$, only the spontaneous decay term survives, leading to a purely dissipative process, which corresponds to the fundamental limiting factor for the coherent evolution of atomic qubits. Noisy dynamics corresponds to the infinite temperature limit, where $\bar{n} \rightarrow \infty$, and, simultaneously, $\Gamma \rightarrow 0$, so that $\Gamma\bar{n} \equiv \tilde{\Gamma}$ is constant. In this case, decay and excitation occur at exactly the same rate, and the noise induced by the transitions between the two levels brings the system to a stationary, maximally mixed state. Finally, a purely dephasing reservoir is obtained by choosing $L_i = d = \sigma_+ \sigma_-$, leading to the master equation

$$\frac{d\rho}{dt} = \frac{\Gamma}{2} (2\sigma_+ \sigma_- \rho \sigma_+ \sigma_- - \sigma_+ \sigma_- \rho - \rho \sigma_+ \sigma_-). \quad (19)$$

In this case, only the off-diagonal elements of the density matrix decay, and phase coherence is lost. This dephasing mechanism is known to be an important source of decoherence in ion traps [35, 36] and in quantum dots experiments [37–39].

If we consider a system of qudits, the operators L_i in Eq. (17) cannot be written anymore in terms of Pauli matrices. To describe the effect of the environment in such systems, we will consider the qudits as two bosonic modes with truncated bases of length d . The terms n and m in the general (pure) state $|\psi\rangle = \sum_{n,m=0}^{d-1} \psi_{nm} |nm\rangle$ then indicate the occupation number in each of these modes. Decay and excitation processes now correspond to the action of annihilation and creation operators a and a^\dagger , analogous to the σ_- and σ_+ for qubits. With this convention, the thermal and dephasing environments are described, respectively, by

$$\mathcal{L}\rho = \frac{\Gamma(\bar{n}+1)}{2} (2a\rho a^\dagger - a^\dagger a \rho - \rho a^\dagger a) + \frac{\Gamma\bar{n}}{2} (2a^\dagger \rho a - a a^\dagger \rho - \rho a a^\dagger), \quad (20)$$

and

$$\mathcal{L}\rho = \frac{\Gamma}{2} (2a^\dagger a \rho a^\dagger a - a^\dagger a \rho - \rho a^\dagger a). \quad (21)$$

Zero and infinite temperature limits are obtained as in the qubit case, and represent, to a very good approximation, the decoherence processes of photons in high- Q cavities [40], and of motional degrees of freedom in ion traps [41].

IV. ENTANGLEMENT DYNAMICS UNDER DECOHERENCE

A. Two qubits case

We shall begin our analysis with the case of two qubits, since it allows for analytical solutions, and can provide some intuition of the processes at work in higher dimensional systems. To provide a more complete and systematic description of the timescales of entanglement decay

under environment interaction, we will recall some known results for the case of dephasing and zero temperature reservoirs, and furthermore derive exact solutions when finite temperature effects are taken into account.

Let us start with initially prepared Bell states $|\Psi^\pm\rangle = (|01\rangle \pm |10\rangle)/\sqrt{2}$, and $|\Phi^\pm\rangle = (|00\rangle \pm |11\rangle)/\sqrt{2}$. Their concurrencies as a function of time are given by

$$c(\Psi^\pm, t) = c(\Phi^\pm, t) = e^{-\Gamma t}, \quad (22)$$

for the dephasing environment, and by

$$c(\Psi^\pm, t) = e^{-\Gamma t}, \quad c(\Phi^\pm, t) = e^{-2\Gamma t}, \quad (23)$$

for the zero temperature case. The first important observation is the accelerated (by a factor of two) decay of concurrence for the Φ^\pm as compared to the Ψ^\pm states, under the influence of a zero temperature environment. This can be understood from the timescales involved in the corresponding solution for the density matrix: while for Ψ^\pm each term $|01\rangle$ and $|10\rangle$ corresponds to a single particle decay, leading to a timescale $e^{-\Gamma t}$, we have the term $|11\rangle$ in Φ^\pm , such that both particles can undergo an environment induced transition to the ground state, thus introducing a faster, $e^{-2\Gamma t}$, decay.

Also for the finite temperature case can an explicit solution be calculated for initial Bell states: it reads

$$c(t) = \max\{c_T(t), 0\}, \quad (24)$$

where the function $c_T(t)$, for Ψ^\pm and Φ^\pm states, is given, respectively, by

$$c_T(\Psi^\pm, t) = \beta - \frac{2(1-\beta)\sqrt{(\bar{n}^2 + \bar{n})^2(\beta+1)^2 + \beta(\bar{n}^2 + \bar{n})}}{(2\bar{n}+1)^2}, \quad (25)$$

and

$$c_T(\Phi^\pm, t) = \beta + \frac{[2\bar{n}(\bar{n}+1) + 1]\beta^2 - \beta - 2\bar{n}(\bar{n}+1)}{(2\bar{n}+1)^2}, \quad (26)$$

with $\beta = e^{-\Gamma(2\bar{n}+1)t}$. These expressions, which reveal the precise role of temperature on the decay of entanglement of Bell states, show that, distinct from the cases of dephasing and zero temperature environments, concurrence does not decay according to a simple mono-exponential law, but rather exhibits various timescales. To apprehend the essential features of temperature effects on entanglement decay, it is useful to focus on the short time limit of these equations [42]. Expanding Eqs. (25) and (26) to first order in t , one finds that the short time concurrence decay is given by

$$c(\Psi^\pm, t) \simeq 1 - \left(2\bar{n} + 1 + 2\sqrt{\bar{n}(\bar{n}+1)}\right) \Gamma t, \quad (27)$$

and

$$c(\Phi^\pm, t) \simeq 1 - 2(2\bar{n} + 1)\Gamma t. \quad (28)$$

This shows that, at the beginning of the evolution, a finite temperature reservoir increases the concurrence decay rate, as compared to the zero temperature case, by a factor of $\left(2\bar{n} + 1 + 2\sqrt{\bar{n}(\bar{n}+1)}\right)$ and of $(2\bar{n} + 1)$, for Ψ^\pm and Φ^\pm states, respectively.

From Eqs. (25) and (26) one can also derive the infinite temperature limit ($\bar{n} \rightarrow \infty$, $\Gamma \rightarrow 0$, with $\Gamma\bar{n} \equiv \tilde{\Gamma} = \text{const.}$) of the thermal bath. In this case, the concurrence becomes

$$c(\Psi^\pm, t) = c(\Phi^\pm, t) = \max\left\{\frac{e^{-4\tilde{\Gamma}t}}{2} + e^{-2\tilde{\Gamma}t} - \frac{1}{2}, 0\right\}. \quad (29)$$

Note that, again, entanglement dynamics involves different timescales. However, a single exponential captures the basic behavior of entanglement decay, since Eq. (29) can be well fitted by a function in the form $\alpha e^{-\gamma t} + \delta$, with negative offset δ . Consequently, separability, i.e. $c(t) = 0$, is reached at finite times for the infinite temperature environment, as well as for any $\bar{n} > 0$. This is in contrast to the above dephasing and zero temperature environments, where separability is reached only asymptotically, and follows from the long-time limit for $c_T(t)$ in Eq. (24)

$$\lim_{t \rightarrow \infty} c_T(t) = -\frac{2\bar{n}(\bar{n}+1)}{(2\bar{n}+1)^2}, \quad (30)$$

which is non-positive for all $\bar{n} > 0$. The exact expressions for this separability time can be easily obtained from the condition $c(t) = 0$, and are of the form $t_{\text{sep}} = \ln[f(\bar{n})]/\Gamma(2\bar{n}+1)$, where the function $f(\bar{n})$ depends on the initial state Ψ^\pm or Φ^\pm . Observe, however, that this is not true for arbitrary initial states. Indeed, some initially mixed states [8] as well as some pure non-maximally entangled states, e.g., $|\psi\rangle = \frac{1}{2}|00\rangle + \frac{1}{2}|01\rangle + \frac{1}{\sqrt{2}}|11\rangle$, reach separability on finite timescales even for a zero temperature environment.

B. Two qudits case

As the dimensions of the subsystems increase, not only a general analytical solution is unknown, but also the numerical approach to obtain reliable estimates of concurrence rapidly turns into a very demanding task. However, it is exactly in this situation where the strength of the tools derived in Section II, for calculating lower bounds of concurrence, becomes manifest. We will devote the remainder of this paper to a systematic analysis of entanglement dynamics in bipartite qudits, using these tools. In particular, we will extract bounds for the *decay rates* of entanglement, and also show how one can infer analytical solutions even for arbitrary dimensions, from the knowledge of the dynamics of the system.

We begin our analysis with the dephasing dynamics described by Eq. (21), which, as discussed in Section III, induces a decay of the off-diagonal elements of the density matrix without changing the diagonal ones. Besides its importance in the description of different physical situations, as already mentioned before, the dephasing model is very instructive since it allows for obtaining analytical solutions for the concurrence of some classes of states. Let us first assume that the initial pure state is of the form $|\psi\rangle = a|m_1 m_2\rangle + b|n_1 n_2\rangle$, what comprises two-level Bell states as special cases. In this situation, one can write the solution of Eq. (21) as

$$\rho(t) = |a|^2|m_1 m_2\rangle\langle m_1 m_2| + |b|^2|n_1 n_2\rangle\langle n_1 n_2| + e^{-\gamma t} ab^*|m_1 m_2\rangle\langle n_1 n_2| + e^{-\gamma t} a^* b|n_1 n_2\rangle\langle m_1 m_2|, \quad (31)$$

with

$$\gamma = \frac{\Gamma}{2} [(m_1 - n_1)^2 + (m_2 - n_2)^2]. \quad (32)$$

Note that there is just one decaying element (and its conjugate) in the density matrix evolution and, therefore, one expects that the entanglement decay rates should follow the same behavior. This is indeed the case, as we will show using the techniques described in Section II: First, one can easily check that the mixed state (31) can be decomposed into contributions of two pure states,

$$|\phi_1\rangle = \sqrt{p}(a|m_1 m_2\rangle + b|n_1 n_2\rangle), \quad (33)$$

and

$$|\phi_2\rangle = \sqrt{1-p}(a|m_1 m_2\rangle - b|n_1 n_2\rangle), \quad (34)$$

with $p = (1 + e^{-\gamma t})/2$, and $\rho = |\phi_1\rangle\langle\phi_1| + |\phi_2\rangle\langle\phi_2|$. From the structure of this decomposition, one can see that, among all $|\chi_\alpha\rangle$, only $|\chi\rangle = (|m_1 n_1\rangle - |n_1 m_1\rangle) \otimes (|m_2 n_2\rangle - |n_2 m_2\rangle)$ gives a non-zero contribution for T^α in Eq. (8). In this case, the concurrence can be expressed in terms of a single matrix T , which reads

$$T = \begin{pmatrix} 2pab & 0 \\ 0 & 2(p-1)ab \end{pmatrix}.$$

Thus the formal structure of two-level systems is retrieved, and the lower bound, Eqs. (10) and (11), is exact. From the singular values of the matrix T , one readily obtains

$$c(t) = 2|ab| e^{(-\Gamma t/2)[(m_1 - n_1)^2 + (m_2 - n_2)^2]}, \quad (35)$$

which is equal to the sum of the absolute values of the two non-vanishing off-diagonal elements of $\rho(t)$.

2. *Zero temperature environment: exact solutions, and estimates*

Although there are no a priori criteria from which to infer the existence of exact solutions like Eq. (35) in general, this is still possible for a large variety of physical

situations. For a zero temperature environment, for example, exact solutions can be derived based on a given form of the decomposition of ρ . Moreover, even if such decomposition does not exist, it is still possible to obtain estimates on the decay rates of concurrence with the tools described in Section II.

To illustrate this, we start with states of the form $|\psi\rangle = a|0m\rangle + b|m0\rangle$ and consider, for the derivation of the exact solution, the case of three-level systems and $a = b = 1/\sqrt{2}$. The decomposition of $\rho(t)$ in terms of its eigenstates (with non-vanishing eigenvalues) reads

$$|\phi_1\rangle = e^{-\Gamma t} (|02\rangle + |20\rangle)/\sqrt{2}, \quad (36)$$

$$|\phi_2\rangle = \sqrt{e^{-\Gamma t}(1 - e^{-\Gamma t})}|01\rangle, \quad (37)$$

$$|\phi_3\rangle = \sqrt{e^{-\Gamma t}(1 - e^{-\Gamma t})}|10\rangle, \quad (38)$$

and

$$|\phi_4\rangle = (1 - e^{-\Gamma t})|00\rangle. \quad (39)$$

All these states, with the exception of $|\phi_1\rangle$, are separable. Therefore, from Eq. (2), one can see that the concurrence of $|\phi_1\rangle$ is an upper bound of $c(\rho)$. Moreover, this term is also the only one that gives a non-vanishing contribution to the matrix $T^{(\text{qp})}$, Eq. (14), in the quasi-pure approximation. Hence, lower and upper bounds coincide and the solution $c(t) = e^{-2\Gamma t}$ is exact. For the state $|\psi\rangle = a|0m\rangle + b|m0\rangle$ the demonstration is analogous, and the concurrence is given by

$$c(t) = 2|ab| e^{-m\Gamma t}. \quad (40)$$

From the time-dependent matrix elements of ρ , which can be obtained from Eq. (20) with $\bar{n} = 0$, one can see that, as in Eq. (35), concurrence is simply given by the sum of the absolute values of the only two non-vanishing off-diagonal elements of ρ . However, we should emphasize that this only happens in special cases alike the present one and, in general, there is no simple relation between the decay of off-diagonal elements of ρ and concurrence.

An example where such a simple relation does not exist, even though an exact solution is possible, is the zero temperature dynamics of initial states of the form $|\psi\rangle = a|00\rangle + b|mm\rangle$. The time-dependent density matrix can be decomposed as $\rho = \xi + \eta$, with η diagonal in the $\{|ij\rangle\}$ basis (and thus separable), and $\xi = \sum \langle ij|\rho|pq\rangle|ij\rangle\langle pq|$ with $i, j, p, q \in \{0, m\}$. From this argument and from Eq.(2) it follows that the concurrence of ξ is an upper bound of $c(\rho)$. Furthermore, ξ is a two-qubit-like matrix and its concurrence can be readily obtained as

$$c(t) = 2e^{-m\Gamma t} \left(|ab| - (1 - e^{-\Gamma t})^m |b|^2 \right). \quad (41)$$

This result coincides with the quasi-pure approximation of $c(\xi)$, calculated using $|\chi\rangle = (|0m\rangle - |m0\rangle) \otimes (|0m\rangle - |m0\rangle)$ in Eqs.(8), (9), (15), and hence is exact.

It is clear from Eq. (41) that the entanglement decay, in this case, encompasses different timescales for $d > 2$, while the only non-zero off-diagonal elements, $\langle 00|\rho|mm\rangle$ and $\langle mm|\rho|00\rangle$, decay as $e^{-m\Gamma t}$. Note also that, in the limit of large m , the concurrence tends to $c(t) = 2|ab|e^{-m\Gamma t}$ and then coincides with the result of Eq. (40). Thus, in this limit, the state $|\psi\rangle = a|00\rangle + b|mm\rangle$ decays as the state $|\psi\rangle = a|0m\rangle + b|m0\rangle$. This shows that the robustness of the Ψ^\pm Bell states as compared to the Φ^\pm in terms of decay rates in the two qubit case (see Eq. (23)) fades away for larger dimensions.

In the two previous examples, exact solutions were possible because ρ could be decomposed into a separable part, and a non-separable two-level-like one whose upper and lower bounds coincide. Although, at first sight, one might judge these conditions to be rather restrictive, the above considerations can be also applied to other environment models and qubit-like initial states. However, what happens when such decomposition does not exist? How much information on the decay rates can we extract with the available tools?

To help to answer these questions let us focus on the situation shown in Fig. 1, where an analytical solution could not be found. For the initial state $|\psi\rangle = (|12\rangle + |21\rangle)/\sqrt{2}$, upper (2) and optimized lower bounds (10, 11), as well as quasi-pure calculations (15), are presented in the upper panel of the figure, as circles, crosses, and squares, respectively. The solid lines represent the quasi-pure approximations for initial states of the form $|\psi\rangle = (|1m\rangle + |m1\rangle)/\sqrt{2}$, with $m = d - 1$ and, from top to bottom, $d = 4$ to $d = 7$. Note that the quasi-pure approximations are calculated only until times when the initially largest eigenvalue λ_1 coincides with the second one (see the lower panel of Fig. 1 for the case $d = 3$). The quasi-pure solutions have a simple form $e^{-(m+1)\Gamma t}$. For $d = 3$, we can go further and use also the numerically calculated upper bound, which in this case is found (through curve fitting) to behave as $e^{-2\Gamma t}$, to confine the actual value of the decay rate to the interval $2\Gamma \leq \gamma \leq 3\Gamma$. Furthermore, we can state that for arbitrary dimensions the decay rate cannot exceed the value given by quasi-pure approximation, which, in the present case, leads to $\gamma \leq d\Gamma$. This is a noticeable asset of our analysis. Even if the high dimension of the system, together with the complex structure of the states, do not allow to determine the precise decay rates of entanglement in the general case, we can extract useful information on their bounds.

3. Finite temperature environment

Finally, let us briefly present a situation where the ability to handle higher dimensional systems is essential: the finite temperature reservoir. Any initial state will evolve asymptotically into a thermal state, which can be described by a finite number of levels – which, however, increases with temperature.

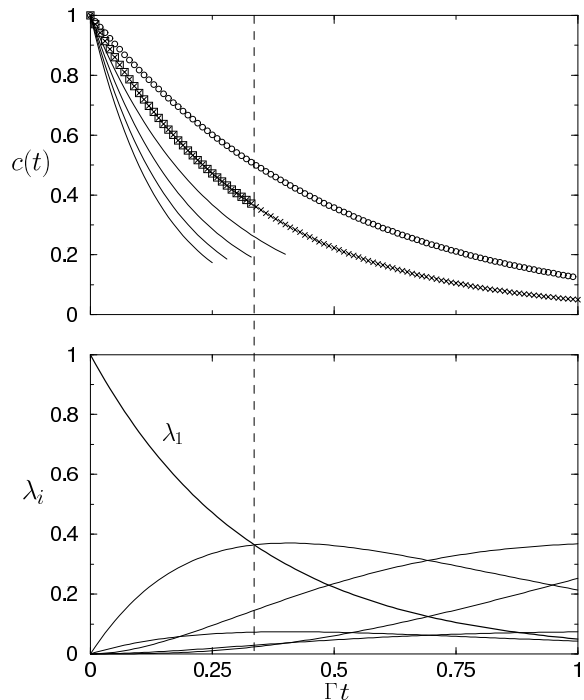


FIG. 1: Top panel: optimized upper (circles) and lower (crosses) bounds of concurrence, as well as quasi-pure approximation (squares), for the initial state $|\psi\rangle = (|12\rangle + |21\rangle)/\sqrt{2}$ coupled to a zero temperature reservoir. The solid lines show the quasi-pure approximations for initial states $|\psi\rangle = (|1m\rangle + |m1\rangle)/\sqrt{2}$, with $m = d - 1$ and, from top to bottom, $d = 4$ to $d = 7$. Quasi-pure solutions behave as $e^{-(m+1)\Gamma t}$ and the upper bound for $d = 3$ is correctly fitted by $e^{-2\Gamma t}$. Bottom panel: eigenvalues of the density matrix $\rho(t)$ as a function of time for $d = 3$. Quasi-pure results coincide with the optimized lower bound and are only calculated while λ_1 remains the largest eigenvalue.

The decoherence effect of this environment on qudits is illustrated in Figure 2, for an initial state $|\psi\rangle = (|01\rangle + |10\rangle)/\sqrt{2}$. The solid, dashed and long-dashed lines represent, respectively, the two qubit solution, Eq. (25), for $\bar{n} = 0.1$, $\bar{n} = 0.2$, and the infinite temperature limit. The corresponding quasi-pure solutions for the same initial state evolving under Eq. (20) are given by circles, squares and crosses. The bold solid curve indicates, for comparison, the zero temperature solution. The dimension used in the simulations ($d = 8$) was chosen to be large enough to describe the dynamics of the system for $\bar{n} = 0.1$ and $\bar{n} = 0.2$, for the times shown in the figure. Note that for the infinite temperature case actually an infinite basis is needed and that our truncated basis set allows for a correct description of the dynamics only for a short period of time ($\bar{\Gamma} t \approx 0.06$), as long as the dynamics do not populate levels at the boundary of the Hilbert space.

The most noticeable effect here is that the expected enhancement of the decay rates with temperature is more pronounced for qudits than for qubits. As a matter of

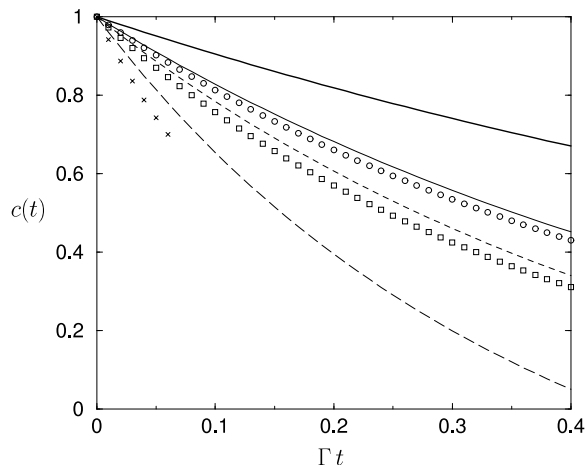


FIG. 2: Finite temperature effects on the decay of entanglement for an initial Bell state Ψ^+ . Solid, dashed and long dashed lines are, respectively, the two-level case solutions of Eq. (18), given by Eq. (25), for $\bar{n} = 0.1$, $\bar{n} = 0.2$, and the infinite temperature limit. Circles, squares and crosses are the corresponding quasi-pure results for the qudits' dynamics given by Eq. (20) using a truncated basis with $d = 8$. For comparison, also the solution for a zero temperature environment is shown (bold line). The expected enhancement of the decay rates with increasing temperature is more pronounced in the higher dimensional case.

fact, this is not too surprising since the dynamics of a finite temperature bath, given by Eq. (20), induces transitions to many different levels, thus speeding up entanglement decay.

V. CONCLUSIONS

In this paper we have contributed to the understanding of the dynamics of entanglement under environment coupling for systems of two qudits. Although no analytical solutions are available in general, we have shown that they can be derived for different classes of initial states and dynamics. Moreover, we have shown how suitable decompositions of the density matrix, together with techniques for calculating lower bounds of concurrence, can be useful to decide on the existence of exact solutions and to derive them for concurrence or its lower bounds. For more general cases in high dimensional systems, we were able to derive upper bounds for the decay rates of entanglement.

Future work will have to focus on error estimates for the employed approximations for concurrence, in higher dimensions.

-
- [1] C. F. Roos, G. P. T. Lancaster, M. Riebe, H. Häffner, W. Hänsel, S. Gulde, C. Becher, J. Eschner, F. Schmidt-Kaler, and R. Blatt, *Phys. Rev. Lett.* **92**, 220402 (2004).
 - [2] C. H. Bennett, H. J. Bernstein, S. Popescu, and B. Schumacher, *Phys. Rev. A* **53**, 2046 (1996).
 - [3] C. H. Bennett, D. P. DiVincenzo, J. A. Smolin, and W. K. Wootters, *Phys. Rev. A* **54**, 3824 (1996).
 - [4] G. Vidal, *J. Mod. Opt.* **47**, 355 (2000).
 - [5] G. Vidal and R. F. Werner, *Phys. Rev. A* **65**, 032314 (2002).
 - [6] T. Yu and J. H. Eberly, *Phys. Rev. B* **66**, 193306 (2002).
 - [7] T. Yu and J. H. Eberly, *Phys. Rev. B* **68**, 165322 (2003).
 - [8] T. Yu and J. H. Eberly, *Phys. Rev. Lett.* **93**, 140404 (2004).
 - [9] F. Mintert, M. Kuś, and A. Buchleitner, *Phys. Rev. Lett.* **92**, 167902 (2004).
 - [10] F. Mintert and A. Buchleitner, *Phys. Rev. A* **72**, 012336 (2005).
 - [11] A. R. R. Carvalho, F. Mintert, and A. Buchleitner, *Phys. Rev. Lett.* **93**, 230501 (2004).
 - [12] M. W. Mitchell, J. S. Lundeen, and A. M. Steinberg, *Nature* **429**, 161 (2004).
 - [13] A. N. Boto, P. Kok, D. S. Abrams, S. L. Braunstein, C. P. Williams, and J. P. Dowling, *Phys. Rev. Lett.* **85**, 2733 (2000).
 - [14] D. Kaszlikowski, P. Gnaniński, M. Żukowski, W. Miklaszewski, and A. Zeilinger, *Phys. Rev. Lett.* **85**, 4418 (2000).
 - [15] D. Collins, N. Gisin, N. Linden, S. Massar, and S. Popescu, *Phys. Rev. Lett.* **88**, 040404 (2002).
 - [16] E. Knill, R. Laflamme, and G. J. Milburn, *Nature* **409**, 46 (2001).
 - [17] S. D. Bartlett, H. de Guise, and B. C. Sanders, *Phys. Rev. A* **65**, 052316 (2002).
 - [18] A. B. Klimov, R. Guzmán, J. C. Retamal, and C. Saavedra, *Phys. Rev. A* **67**, 62313 (2003).
 - [19] M. F. Santos, *Phys. Rev. Lett.* **95**, 010504 (2005).
 - [20] H. Bechmann-Pasquinucci and A. Peres, *Phys. Rev. Lett.* **85**, 3313 (2000).
 - [21] M. Bourennane, A. Karlsson, and G. Björk, *Phys. Rev. A* **64**, 012306 (2001).
 - [22] N. J. Cerf, M. Bourennane, A. Karlsson, and N. Gisin, *Phys. Rev. Lett.* **88**, 127902 (2002).
 - [23] T. Durt, N. J. Cerf, N. Gisin, and M. Żukowski, *Phys. Rev. A* **67**, 012311 (2003).
 - [24] A. Mair, A. Vaziri, G. Weihs, and A. Zeilinger, *Nature* **412**, 313 (2001).
 - [25] A. Lamas-Linares, J. C. Howell, and D. Bouwmeester, *Nature* **412**, 887 (2001).
 - [26] J. C. Howell, A. Lamas-Linares, and D. Bouwmeester, *Phys. Rev. Lett.* **88**, 030401 (2002).
 - [27] A. Vaziri, G. Weihs, and A. Zeilinger, *Phys. Rev. Lett.* **89**, 240401 (2002).
 - [28] R. T. Thew, A. Acín, H. Zbinden, and N. Gisin, *Phys. Rev. Lett.* **93**, 010503 (2004).
 - [29] H. S. Eisenberg, G. Khoury, G. Durkin, C. Simon, and D. Bouwmeester, *Phys. Rev. Lett.* **93**, 193901 (2004).
 - [30] L. Neves, G. Lima, J. G. A. Gómez, C. H. Monken,

- C. Saavedra, and S. Pádua, Phys. Rev. Lett. **94**, 100501 (2005).
- [31] W. K. Wootters, Phys. Rev. Lett. **80**, 2245 (1998).
- [32] P. Rungta, V. Buzek, C. M. Caves, M. Hillery, and G. J. Milburn, Phys. Rev. A **64**, 042315 (2001).
- [33] F. Mintert, , M. Kuś, and A. Buchleitner, quant-ph/0411127.
- [34] F. Mintert, A. R. R. Carvalho, M. Kuś, and A. Buchleitner, Phys. Rep. **415**, 207 (2005).
- [35] C. Monroe, D. M. Meekhof, B. E. King, W. M. Itano, and D. J. Wineland, Phys. Rev. Lett. **75**, 4714 (1995).
- [36] R. Blatt, H. Häffner, C. F. Roos, C. Becher, and F. Schmidt-Kaler, Quant. Inf. Process. **3**, 61 (2004).
- [37] J. M. Taylor, C. M. Marcus, and M. D. Lukin, Phys. Rev. Lett. **90**, 206803 (2003).
- [38] T. Hayashi, T. Fujisawa, H. D. Cheong, Y. H. Jeong, and Y. Hirayama, Phys. Rev. Lett. **91**, 226804 (2003).
- [39] T. Itakura and Y. Tokura, Phys. Rev. B **67**, 195320 (2003).
- [40] M. Brune, E. Hagley, J. Dreyer, X. Maître, A. Maali, C. Wunderlich, J. M. Raimond, and S. Haroche, Phys. Rev. Lett. **77**, 4887 (1996).
- [41] Q. A. Turchette, C. J. Myatt, B. E. King, C. A. Sackett, D. Kielpinski, W. M. Itano, C. Monroe, and D. J. Wineland, Phys. Rev. A **62**, 053807 (2000).
- [42] R. Guzmán, J. C. Retamal, J. L. Romero, and C. Saavedra, Phys. Lett. A **323**, 382 (2004).
- [43] Note that $|\chi_\alpha\rangle \in \mathcal{H}_1 \otimes \mathcal{H}_1 \otimes \mathcal{H}_2 \otimes \mathcal{H}_2$, whereas $|\phi_j\rangle \otimes |\phi_k\rangle \in \mathcal{H}_1 \otimes \mathcal{H}_2 \otimes \mathcal{H}_1 \otimes \mathcal{H}_2$. Nevertheless, the two spaces are isomorphic, and it is straightforward to identify the correspondence between their elements.